Altered glycosylation patterns increase immunogenicity of a subunit HCV vaccine inducing neutralizing antibodies which confer protection in mice

Dapeng Li[1], Markus von Schaewen[2], Xuesong Wang[3], Wanyin Tao[3], Yunfang Zhang[1], Li Li[3], Brigitte Heller[2], Gabriela Hrebikova[2], Qiang Deng[1], Alexander Ploss[2#], Jin Zhong[3*#], Zhong Huang[1*#]

[1] Vaccine Research Center, CAS Key Laboratory of Molecular Virology & Immunology, Institut Pasteur of Shanghai, Chinese Academy of Sciences, Shanghai 200031, China.

[2] Department of Molecular Biology, Princeton University, Princeton, New Jersey 08544, USA.

[3] Unit of Viral Hepatitis, CAS Key Laboratory of Molecular Virology & Immunology, Institut Pasteur of Shanghai, Chinese Academy of Sciences, Shanghai 200031, China.

*To whom correspondence should be addressed: huangzhong@ips.ac.cn (Z.H.); jzhong@sibs.ac.cn (J.Z.).

[#]Z.H., J.Z. And A.P. are co-senior authors of the paper.

Running title: A subunit HCV vaccine produced in insect cells

Abstract:

Hepatitis C virus (HCV) infection is a global health problem for which no vaccine is available. HCV has a highly heterogeneous RNA genome and can be classified into seven genotypes. Due to the high genetic and resultant antigenic variation among genotypes, inducing antibodies capable of neutralizing most of the HCV genotypes by experimental vaccination has been challenging. Previous efforts focused on priming humoral immune responses with recombinant HCV envelope E2 protein produced in mammalian cells. Here, we report that a soluble form of HCV E2 (sE2) produced in insect cells possess different glycosylation patterns and is more immunogenic as evidenced by the induction of higher titers of broadly neutralizing antibodies (bNAbs) against cell culture-derived HCV (HCVcc) harboring structural proteins from a diverse array of HCV genotypes. We affirm that continuous and discontinuous epitopes of well-characterized bNAbs are conserved, thus suggesting that sE2 produced in insect cells is properly folded. In a genetically humanized mouse model, active immunization with sE2 efficiently protected against challenge with a heterologous HCV genotype. These data not only demonstrate that sE2 is a promising HCV vaccine candidate but also highlight the importance of glycosylation patterns in developing subunit viral vaccines.

Importance:

A prophylactic vaccine with high efficacy and low cost is greatly needed for global control of HCV infection. Induction of broadly neutralizing antibodies against most HCV genotypes has been challenging due to the antigenic diversity of the HCV genome. Herein, we refined a high-yield subunit HCV vaccine that elicited broadly neutralizing antibody responses in preclinical trials. We found that soluble HCV E2 protein (sE2) produced in insect cells is distinctly glycosylated and is more immunogenic than sE2 produced in mammalian cells, suggesting that glycosylation patterns should be taken into consideration in efforts to generate antibody-based, recombinant vaccines against HCV. We further showed that sE2 vaccination confers protection against HCV infection in a genetically humanized mouse model. Thus our work identified a promising broadly protective HCV vaccine candidate, which should be considered of further pre-clinical and clinical development.

Introduction

It is estimated that over 2% of the world's population is chronically infected with hepatitis C virus (HCV) (1). Although recently approved direct-acting antiviral (DAA) drugs (2) have greatly improved upon the curing efficacy of the previous interferon (IFN)-based regimen, these new therapies are very expensive and thus unaffordable for the majority of HCV-infected individuals who live in developing countries where most new infections occur. Since the approval of these highly effective DAAs, the number of chronic HCV carriers has not significantly declined. Furthermore, there is little evidence that patients cured of their chronic infection with DAAs retain antiviral immunity that is protective against future HCV exposures. Therefore, the development of a prophylactic HCV vaccine with high efficacy and low cost remains a high priority in the global control of HCV infection. Natural clearance of HCV correlates with the induction of vigorous T cell responses with broad specificity, which has prompted efforts to pursue T cell based vaccines. Currently, the only vaccine candidate in clinical trials is based on the expression of HCV non-structural proteins with adenoviruses and MVA to elicit T cell responses to infection (3, 4).

However, T cell based vaccines cannot prevent the first steps of a viral infection, thus creating a rational for alternative/addition approaches geared towards induction of neutralizing antibodies (NAbs) which could putatively block HCV uptake. NAbs have been found to correlate with the protection offered by all viral vaccines licensed thus far (5). However, the role of anti-HCV antibodies in humans is under debate. A strong correlation between viral clearance and the induction of an early and broad NAb response following HCV infection has been reported in a number of patient cohorts with HCV infection (6-8). In addition,

in vivo challenge/protection studies have shown that the passive transfer of monoclonal and polyclonal NAbs was able to prevent HCV infection in chimpanzees (9) and in mice (10-14), highlighting the important role of NAbs in protecting against HCV infection. A single HCV vaccine that could induce NAbs against all the known seven HCV genotypes would be ideal. However, due to the extreme genetic and antigenic diversity across and within HCV genotypes, this has been a particularly challenging goal (15).

The HCV envelope proteins E1 and E2 are responsible for mediating HCV entry into target cells by direct or indirect interaction with numerous host molecules (16, 17) and are thus the natural targets of NAbs (18). Consequently, all experimental HCV vaccines that aim to generate NAbs contain E2 and/or E1 components in a variety of modalities or prime-boost regimens (19-28). Although significant progress has been made towards the development of an efficacious HCV vaccine mediating protection by inducing humoral immune responses, several important issues remain: (i) the spectrum of NAbs elicited by existing vaccine candidates is still insufficiently broad to cover all seven HCV genotypes; (ii) the complexity of the heterologous prime-boost regimens with different antigen modalities renders vaccine production and vaccination difficult; (iii) the low yield of antigen manufacture hampers the application for some promising vaccine candidates, such as inactivated cell culture-derived HCV (HCVcc) (23); (iv) few of these vaccines have been evaluated in an immunocompetent animal model by active immunization as the utilization of chimpanzees is limited for ethical and financial reasons and murine models such as human liver chimeric mice (29) are immunodeficient. To address some of these challenges, we aimed to develop an improved method for inducing bNAbs. We demonstrate that expression of a transmembrane

domain-truncated, soluble version of E2 (designated sE2) in insect cells results in an antigen with increased immunogenicity as compared to equivalent constructs produced in mammalian cells. Mice mount strong immune responses to sE2, yielding high titers of anti-HCV E2 antibodies capable of neutralizing a diverse panel of HCV intergenotypic chimeras *in vitro*. Following sE2 vaccination, genetically humanized mice were protected against experimental challenge with a heterologous HCV strain.

Materials and Methods

Establishment of HCVcc panels covering genotypes 1-7

A panel of HCVcc covering genotypes 1 to 7 was used for the neutralization assay. All these HCVcc were produced following a protocol previously described (30) including *in vitro* transcription, HCV RNA electroporation, immunostaining, HCVcc titration and amplification. Plasmids pUC-Con1/JFH1, pUC-H77/JFH1, and pUC-J6/JFH1 were constructed as previously described (31). Plasmids pJ8/JFH1, pS52/JFH1 (I793S, K1404Q), pED43/JFH1 (T827A, T977S), pSA13/JFH1 (A1022G, K1119R), pHK6a/JFH1 (F350S, N417T) and pQC69/JFH1 were generously provided by Dr. Jens Bukh at University of Copenhagen (32). The chimeric genotype 1b HCVcc (PR52B6Mt and PR79L9) constructed from clinical isolates was reported previously (33).

Construction of expression plasmids

We amplified optimized sE2 (aa. 384-661) from codon-optimized HCV E2 gene (Con1 strain, genotype 1b, optimized and synthesized by GeneArt) with forward primer

NcoI-sE2opti-F (5' CTGCCATGGCCGGCACATACGTGACAG 3') and reverse primer sE2opti-XbaI-R (5' GCACTCTAGACTCGCTTCTGTCCCGAT 3'), then inserted the PCR product into the vector pMT/BiP/V5-HisA (Invitrogen) to obtain pMT-sE2. To produce a sE2 without HVR1, we used the same approach (forward primer NcoI-ΔHVR1-F: 5' GCCCCATGGCAGCTGGTGAACACCAACGGCAGC 3'; reverse primer sE2opti-XbaI-R) to obtain pMT-sE2ΔHVR1. To generate the mammalian sE2, the whole open reading frame (including gene encoding the signal peptide and tags) was cloned from pMT-sE2 into pcDNA3.1 vector (forward primer: 5' CCCGCTAGCGCCACCATGAAGTTATGCATATTACTG GCCGTCG 3'; reverse primer: 5' CCCGAATTCTCAATGGTGATGGTGATGATGACCGGTAC 3') to obtain pcDNA3.1-sE2. To express the extracellular loop of human CD81 (hCD81LEL, aa. 112-202), we amplified the hCD81LEL gene from the construct pLEGFP-CD81(34) by PCR (forward primer hCD81LEL-F-NcoI: 5' CAGCCATGGGCTTTGTCAACAAGGACCAG 3'; reverse primer hCD81LEL-R-XhoI: 5' GAACTCGAGCAGCTTCCCGGAGAAGAGGTC 3') and inserted the fragment into pET26b, to yield pET26b-hCD81LEL. All plasmids constructed were verified by DNA sequencing.

Expression and Purification of sE2 from stable Drosophila S2 cell clones

To generate stable transfectants expressing sE2, we co-transfected S2 cells with pMT-sE2 and a selection vector pCoBlast, followed by blasticidin screening. S2 cells cultured in complete Schneider's *Drosophila* Media (SDM; Gibco) supplemented with 10% fetal bovine serum (FBS; Gibco), 100 U/ml of penicillin/streptomycin (Gibco), and 100 mg/L of L-glutamine (Gibco) were seeded at 3×10^6 cells/well in a 6-well plate. After 12 h, we co-transfected 19 μg

pMT-sE2 and 1 μg selection vector pCoBlast by calcium phosphate transfection and changed the medium after 16-24 h of incubation. Seventy-two hours post-transfection, we changed the medium to complete SDM containing 25 μg/ml blasticidin. After 1-2 weeks of selection, the medium was changed again with complete SDM containing 10 μg/ml blasticidin. To generate stable, high-yield cell clones, we seeded 1.5 cells/well of the stable transfected cells into 96-well plates. After 2-weeks of selection with SDM containing 10 μg/ml blasticidin, we detected sE2 expression from supernatants of each well by ELISA and Western blot. Several monoclonal cells with high-yields of sE2 were obtained. We chose one clone named sE2B3 for the following large-scale culture and expression. For large-scale expression, sE2B3 cells were cultured in complete Express Five SFM medium (SFM; Gibco) supplemented with 100 U/ml of penicillin/streptomycin, 100 mg/L of L-glutamine and 10 μg/ml blasticidin, in a 3L Spinner Flask (Bellco). When cell concentration reached 2×10^7 cells/ml, cells were induced with chromic chloride at a final concentration of 5 μM. On day five post-induction, the supernatant was harvested and concentrated to a volume of 50-100 ml in binding buffer (0.5 M NaCl, 20 mM Tris, 10 mM imidazole, pH 7.9) by ultrafiltration in a stirred cell (Amicon 8400, Millipore) through a 5-kDa membrane. Then sE2 proteins were purified from the concentrated supernatant using Ni-NTA resins (Novagen) according to the manufacturer's instructions. The eluted sE2 proteins were analyzed by SDS-PAGE (12% acrylamide) and Western blot. To obtain highly pure sE2 as a stimulus for ELISPOT assays, the Ni-NTA purified proteins were subjected to size exclusion chromatography using a Superdex 200 10/300 GL column (GE Healthcare). The HVR1 deleted form, sE2ΔHVR1, was expressed and purified using the same protocol.

160

161 **Expression and Purification of sE2 from HEK293T cells**

162 To generate sE2 from mammalian cells, HEK293T cells cultured in complete Dulbecco's
163 modified Eagle medium (DMEM; HyClone) supplemented with 10% FBS, 10 mM HEPES
164 buffer (Gibco), 100 mg/L of L-glutamine, 1% non-essential amino acids (NEAA; Gibco) and
165 100 U/ml penicillin/streptomycin were transfected with pcDNA3.1-sE2 using branched
166 Polyethylenimine (PEI; Sigma-Aldrich). Medium containing PEI was changed with complete
167 DMED with 10μM sodium butyrate at 4h post-transfection, and then changed with FreeStyle
168 293 Medium (FS293, Gibco) 12h later. Mammalian sE2 were harvested, concentrated and
169 purified from the medium harvested 72h post transfection following the same protocol
170 described above.

171

172 **Deglycosylation of sE2**

173 Under a reducing condition, 10 μg of sE2 protein was denatured at 100°C for 10 min in
174 1X Glycoprotein Denaturing Buffer, and then digested by PNGase F (200U) or Endo H (200U)
175 at 37°C for 1 h according to the manufacturer's instructions (New England Biolabs). The
176 deglycosylated protein was analyzed by Western blotting. Under a non-reducing condition,
177 sE2 dissolved in PBS was digested by PNGase F at 4°C overnight. The resulting
178 N-deglycosylated sE2 was purified by Ni-NTA resin and applied to ELISA, receptor-binding
179 assay and immunization experiments.

180

181 **SDS-PAGE and Western Blot Assay**

182 Induced cell supernatants or purified sE2 proteins were separated on a 12% SDS-PAGE
183 gel and stained with Coomassie brilliant blue G-250 or transferred onto polyvinylidene
184 difluoride membranes (PVDF; Pall). The membrane was probed with an anti-His tag mAb
185 (1:1,000 dilution; M30111; Abmart) or anti-E2 mAb AP33 (35) (1:1,000 dilution; kindly
186 provided by Dr. Arvind Patel at MRC - University of Glasgow), followed by a corresponding
187 secondary antibody.
188
189 **ELISA**
190 To determine the antigenicity of sE2, 96-well EIA/RIA flat-bottom plates (Costar, Corning,
191 NY, USA) were coated overnight with serially diluted sE2. The plates were blocked with PBST
192 containing 5% nonfat dry milk for 1 h at 37°C. E2 mAbs AR3A (kindly provided by Drs.
193 Mansun Law and Denis Burton at the Scripps Research Institute) or AP33 (35) were then
194 added, followed by incubation for 2 h at 37°C. Then, horseradish peroxidase
195 (HRP)-conjugated anti-human IgG antibody (1:5,000 dilution; ab6858; Abcam) or
196 HRP-conjugated anti-mouse IgG antibody (1:5,000 dilution; 31432; Invitrogen) was added
197 and incubated for 1 h. After color development, colorimetric analysis was performed at 450
198 nm in a 96-well plate reader.
199
200 **Receptor-binding assay**
201 The receptor-binding assay to analyze the capacity of sE2 binding to HCV entry factors
202 has been previously described (34). Briefly, 100 μg of purified sE2 protein was incubated with
203 parental CHO cells or with CHO cells expressing SR-BI or CD81 at 37°C for 1 h. After

washing with PBS, the cells were incubated with anti-His mouse monoclonal antibody on ice for 1 h, and then with Alexa Fluor 555-conjugated donkey anti-mouse IgG (1:200; A31570; Molecular Probes), followed by flow cytometry analysis on a BD LSRII flow cytometer (BD Biosciences, San Diego, CA). The results were analyzed with FlowJo software.

Human CD81LEL protein was expressed and purified to compete the binding of sE2. Briefly, pET26b-hCD81LEL was transformed into BL21 competent cells. Soluble hCD81LEL was obtained by a low temperature induction and purified using Ni-NTA resins according to the manufacturer's instructions. In the CD81LEL competitive inhibition assay, sE2 was incubated with different doses (200 μg, 20 μg and 2 μg) of CD81LEL at 37°C for 1 h, following by the receptor-binding assay described above.

HCV infection-blocking assay

To perform an HCV infection-blocking assay, Huh-7.5.1 cells cultured in complete DMEM were seeded at 1×10^4 cells/well in a 96-well plate for 12 h. Then, approximately 4×10^3 FFU/ml of Con1/JFH1 chimeric HCVcc was mixed with serially diluted sE2 protein, CD81LEL protein or bovine serum albumin (BSA; New England Biolabs), and added to the Huh-7.5.1 cells. After 4 h, the protein-virus mixture was changed to complete DMEM. After 72 h of culture, immunostaining was performed as previously described (36) with some modifications. Briefly, cells were fixed with fixation buffer (4% paraformaldehyde in PBS) and blocked with blocking buffer (3% BSA, 0.3% Triton X-100 and 10% FBS in PBS), followed by incubation with anti-HCV NS5A mAb (1:1,000 dilution; Abmart, Shanghai), with Alexa Fluor 488-conjugated donkey anti-mouse IgG (1:1,000 dilution; A21202; Molecular Probes) and Hoechst dye

(1:10,000 dilution; Molecular Probes). The fluorescent foci were observed and enumerated on a standard fluorescent microscope (Leica).

Animal immunization

Balb/c mice were purchased from Shanghai SLAC Laboratory Animal Inc. Prior to immunization, 50 μg sE2 antigens were formulated with 1 mg Inject Alum (Pierce), 1 mg Inject Alum plus 25 μg CpG 7909 (also known as CpG2006 or PF-3512676; 5' TCGTCGTTTTGTCGTTTTGTCGTT 3', synthesized from Sangon Biotech, Shanghai), or FA (Complete FA for prime, and Incomplete FA for boost; Sigma-Aldrich) at a volumetric ratio of 1:1 according to the manufacturer's instructions. To test the capacity of sE2-inducing NAbs, groups of ten female Balb/c mice (6-week old) were injected intraperitoneally (i.p.) at weeks 0, 2 and 4. Blood samples were collected at weeks 0, 2, 4, 6, 13, 17, 22 and 25. To test sE2-induced immune memory, we boosted mice at week 25 when serum titers significantly decreased and performed blood sampling at weeks 27 and 28, when mice were terminated. Sera were kept at −80°C until use. To compare insect cell-derived sE2 and mammalian cell-derived sE2, and to compare sE2 and sE2ΔHVR1, groups of six female Balb/c mice (6-week old) were i.p. injected at weeks 0, 2, 4 and 6. Blood samples were collected every two weeks. In a separate experiment, each of the three sE2 samples representing different oligomeric states were formulated with alum and used for mouse immunization (6 mice/group) with the same dosage and immunization schedule as described above, and mouse antisera were collected at week 12 for measurement of neutralization activities against HCVcc. All the animal immunization studies were approved by the Institutional Animal Care and Use

248 Committee at the Institut Pasteur of Shanghai (protocol number: A2013006). The animals
249 were cared for in accordance with institutional guidelines.
250
251 **Antibody measurement**
252 To measure E2-specific antibody responses in serum samples by ELISA, 96-well
253 EIA/RIA flat-bottom plates were coated overnight with 100 ng/well of sE2. After blocking,
254 serially diluted sera from mice were added as primary antibodies, followed by 1:5,000 diluted
255 HRP-conjugated anti-mouse IgG antibody. After color development, colorimetric analysis was
256 performed at 450 nm in a 96-well plate reader. For a given serum sample, endpoint titer was
257 defined as the the reciprocal of the highest serum dilution that had an absorbance >0.1 OD
258 unit above that of the pre-immune samples. For computation of geometric mean titers (GMTs),
259 serum samples that did not yield positive readings at the lowest dilution tested (1:100) were
260 assigned an endpoint titer of 50.
261 For measurement of sE2-specific IgG1 and IgG2a responses, sera from each mouse
262 were 1:10,000 diluted, and then subjected to ELISA analysis using the above described
263 protocol with some modifications: HRP-conjugated goat anti-mouse IgG1 and goat
264 anti-mouse IgG2a (SouthernBiotech) were used as the secondary antibody, respectively. The
265 ratio of IgG1 and IgG2a isotypes was calculated by dividing OD values for IgG1 with OD
266 values for IgG2a.
267
268 **Competitive ELISA**

HRP-conjugated AP33 and AR3A antibodies were generated, respectively, by using EZ-Link Plus Activated Peroxidase Kit (Thermo Fisher Scientific). For the competitive ELISA, 96-well EIA/RIA flat-bottom plates were coated overnight with 100 ng/well of sE2. After blocking, serially diluted mouse antisera were added to the wells and incubated at 37°C for 1 h, followed by three washes with PBS. Then, HRP-conjugated AP33 (2 μg/mL) or HRP-conjugated AR3A (2 μg/mL) was added to the wells and incubated at 37°C for 1 h. After color development, colorimetric analysis was performed at 450 nm in a 96-well plate reader.

Measurement of neutralization activity of the antisera

A panel of HCVcc covering genotypes 1 to 7 was established. All these HCVcc were used in neutralization assays to assess the neutralization breadth of the antisera. Briefly, serum samples were heat-inactivated at 56°C for 1 h, and diluted to their appropriate dilutions in complete DMEM. HCVcc were diluted in complete DMEM to approximately 4×10^3 foci forming units (FFU)/ml, mixed with equal volume (50 μl) of diluted serum samples, and incubated at 37°C for 2 h. The virus-serum mixture was transferred to Huh-7.5.1 cells seeded 12 h previously in 96-well plates (1×10^4 cells/well) and replaced with complete DMEM after 4-6 h of incubation at 37°C. The cells were incubated at 37°C for 72 h, followed by fixing and NS5A-immunostaining. Percent neutralization was calculated by comparing the focus numbers of immune serum to that of a pre-immune serum control at the same dilutions.

Measurement of cellular immune responses by ELISPOT assay

To determine the IFN-γ- and Interleukin-4- (IL-4) secreting cells in splenocytes, 96-well PVDF plates (Millipore) were pre-coated with anti-mouse IFN-γ capture antibody (an-18; eBiosciences) or anti-mouse IL-4 capture antibody (11B11; eBiosciences) at 4°C overnight. Plates were blocked with complete RPMI-1640 medium (Gibco) for 1h at 37°C and freshly isolated splenocytes were added to the plates. sE2, medium (negative control) or concanavalin A (positive control) was diluted in complete RPMI-1640 medium and added to each well at a final concentration of 10 μg/ml and incubated for 48h at 37°C and 5% CO_2. Subsequently, the plates were incubated with biotinylated anti-mouse IFN-γ detection antibody (R4-6A2; eBiosciences) or biotinylated anti-mouse IL-4 detection antibody (BVD6-24G2; eBiosciences) diluted in PBST for 2 h, and then with AP-conjugated streptavidin (Mabtech) diluted in PBS for 1 h. After washing, NBT/BCIP substrate (Promega) was added for color development. The cytokine-secreting cell spots were imaged and counted on a CTL Immunospot reader (Cellular Technology Ltd.).

Determination of Oligomeric state

Ni-NTA-purified sE2 was subjected to size exclusion chromatography (SEC) using the AKTA Fast Protein Liquid Chromatography (FPLC) system. Briefly, sE2 was loaded on a Superdex 200 10/300 GL column, and SEC was performed in PBS buffer at flow rate of 0.5 ml/min. The eluent was analyzed by SDS-PAGE under reducing or non-reducing conditions. For the non-reducing SDS-PAGE, protein samples were mixed with sample buffer without β-mercaptoethanol and loaded into the gel without boiling.

Generation of recombinant HCV

Construction of BiCre-Jc1 encoding recombinase Cre is described elsewhere(12). Briefly, the plasmid encoding BiCre-Jc1 was linearized with Xba I and transcribed using MEGAscript T7 (Ambion). RNA was electroporated into Huh-7.5 cells using an ECM 830 electroporator (BTX Genetronics). The transfected Huh-7.5 cells were cultured in complete DMEM until 72 hours after electroporation, when the medium was replaced with serum-free DMEM and supernatants were harvested every 6 hours for 3 days. Supernatants were pooled, filtered through a 0.45 μm bottle top filter (Millipore), and concentrated using a stirred cell (Millipore). Viral titers ($TCID_{50}$) were determined using Huh-7.5 cells as previously described (37).

Generation and production of recombinant adenovirus

Adenovirus encoding human homologs of the two species-specific HCV entry factors CD81 and OCLN (AdV-hCD81-2A-hOCLN) was constructed via overlapping PCR of hCD81 and hOCLN templates and cloned into pShuttle. The pSh-hCD81-2A-hOCLN was then electroporated into BJ5183 AD-1 cells (Agilent), which were pre-transformed with pAdEasy-1 to facilitate recombination with the pShuttle vector. Colonies were selected, prepped, and screened for a 3-kb band following PacI digestion.

Adenovirus constructs were then transfected into HEK293 cells (American Type Culture Collection) cultured in complete DMEM using the calcium phosphate method. Transfected cultures were maintained until cells exhibited complete cytopathic effect (CPE), then harvested, and freeze-thawed. Supernatants were serially passaged two more times with harvest at complete CPE and freeze-thaw. For virus purification, cell pellets were

resuspended in 0.01 M sodium phosphate buffer (pH 7.2) and lysed in 5% sodium deoxycholate, followed by DNase I digestion. Lysates were centrifuged, and the supernatant was layered onto a CsCl gradient (1.2 to 1.46 g/ml) and spun at 23,000 rpm in a Beckman Optima 100K Ultracentrifuge using an SW28 spinning bucket rotor (Beckman Coulter). Adenovirus bands were isolated and further purified on a second CsCl gradient using an SW41 spinning bucket rotor. Resulting purified adenoviral bands were isolated using an 18.5-gauge needle and twice-dialyzed against 4% sucrose. Adenovirus concentrations were measured at 10^{12} times the dilution factor times the OD260 reading on a Nanodrop 2000 (Thermo Fisher Scientific). Adenovirus stocks were aliquoted and stored at −80°C.

Active immunization and bioluminescence imaging

Gt(ROSA)26Sor$^{tm1(Luc)Kaelin}$ mice (Rosa26-Fluc) were obtained from The Jackson Laboratory. Mice were bred and maintained at the Laboratory Animal Resources of Princeton University according to guidelines established by the Institutional Animal Committee (Protocol number 1930). After sE2 immunization, Rosa26-Fluc mice were injected with 10^{11} adenovirus particles 24 hours before intravenous injection with $2x10^{7}$ $TCID_{50}$ HCV-BiCre-Jc1. At 72 hours post-infection, mice were anesthetized using an isoflurane inhalation anesthesia and injected intraperitoneally with 1.5 mg of D-luciferin (Caliper Life Sciences). Bioluminescence was measured using an IVIS Lumina II platform (Caliper Life Sciences).

Statistics

355 Significance comparisons were calculated with two-tailed student *t* test or Kruskal-Wallis
356 One-Way ANOVA analysis. For correlations, a nonparametric Spearman's test was used.
357 Significance values are shown as: not significant (ns) $P \geq 0.05$, * $P < 0.05$, ** $P < 0.01$, ***
358 $P < 0.001$ and **** $P < 0.0001$. All statistical analyses were performed on GraphPad Prism 5.0c
359 (GraphPad Software, CA).
360
361
362 **Results**
363 **High-yield production of soluble E2 glycoprotein in *Drosophila* S2 Cells**
364 Previous efforts to develop a recombinant HCV vaccine relied on expression of E2 or
365 E1/E2 heterodimer in mammalian cells (27, 28, 38-40). It was reported that N-glycans
366 associated with HCV E2 could modulate receptor-binding affinity as well as neutralizing
367 epitope recognition (41). Thus, we hypothesized that glycosylation might influence the
368 antigenicity and immunogenicity of sE2. To directly determine the contribution of glycosylation
369 on the induction of bNAbs by sE2, we produced sE2 in mammalian and insect cell lines
370 known to yield altered glycan structures on proteins (42). To produce E2 protein of the HCV
371 strain Con1 (genotype 1b) in insect cells, we used an established *Drosophila* S2 cell
372 expression system (43). Transgenic cell lines expressing sE2 comprised of residues 384-661
373 were recovered following transfection of *Drosophila* S2 cells with pMT-sE2 and subsequent
374 antibiotic selection (Fig. 1A). The sE2 protein was secreted into cell culture supernatant and
375 remained stable for at least nine days (Fig. 1B). sE2 was readily purified from cell culture
376 supernatant to near homogeneity (Fig. 1C) at high levels of up to 100 mg/L of supernatant.

377 The purified sE2 migrated at ~45kDa (Fig. 1C), which is much higher than the predicted mass
378 (~34kDa) based on its amino acid sequence, suggesting possible glycosylation. To examine
379 the extent and pattern of glycosylation, sE2 was digested with endoglycosidases Endo H and
380 PNGase F. As shown in Fig. 1D, PNGase F treatment of sE2 generated a band at the
381 calculated molecular mass of ~34 kDa, suggesting that sE2 is fully deglycosylated by
382 PNGase F. Endo H digestion resulted in a band only slightly below untreated sE2, suggesting
383 that sE2 contains Endo H-resistant glycan types, such as paucimannose N-glycans, as
384 previously reported for other S2 cell-produced glycoproteins (42).
385
386 **Functional and conformational characterization of sE2**
387 Proper folding of recombinant sE2 is critical for inducing antibodies capable of binding to
388 the envelope of HCV particles. Thus, we performed a variety of tests to insure that sE2 retains
389 its native conformation. CD81 and SRB1 are two critical HCV entry factors and directly
390 interact with E2 (44, 45), but only when the E2 protein is properly folded. To determine
391 whether S2 cell-produced sE2 can bind CD81 and SRB1, CHO cells stably expressing human
392 CD81 (designated CHO-CD81) or SRB1 (CHO-SRB1) were incubated with sE2, and the
393 binding of sE2 to CHO-CD81 or CHO-SRB1 cells assessed by flow cytometry (34). As shown
394 in Fig. 1E, sE2 bound to both CHO-CD81 and CHO-SRB1, and binding to CHO-CD81 was
395 inhibited by recombinant soluble large extracellular loop of CD81 (CD81LEL) in a
396 dose-dependent manner (Fig. 1F) in agreement with the previous finding that CD81LEL is the
397 binding domain of E2 (45). Next, we tested sE2 for its ability to block HCVcc infection. As
398 shown in Fig. 1G, HCVcc infection of Huh-7.5.1 cells was inhibited by sE2 in a

399 dose-dependent manner, demonstrating that sE2 competes with HCVcc for receptor binding
400 sites.

401 The conformation of sE2 was further assessed by using two well-characterized,
402 E2-specific, broadly neutralizing monoclonal antibodies (mAbs) AR3A (10) and AP33 (35),
403 which target conformational and linear epitopes, respectively. ELISA analysis revealed that
404 sE2 efficiently reacted with both AR3A and AP33 in a dose-dependent manner (Fig. 1H).
405 Because AR3A recognizes a conformational epitope that overlaps with the CD81 binding site
406 (10, 46), our results demonstrate that sE2 acquires a conformation critical for binding both key
407 receptors and bNAbs, and therefore has a high potential to elicit bNAbs. Thus, collectively,
408 our data strongly suggest that our sE2 antigen is properly folded.
409

410 **Immunization of mice with sE2 induces HCV E2-specific antibodies that can neutralize**
411 **a diverse panel of HCV genotypes**

412 The immunogenicity of our recombinant sE2 vaccine was first evaluated in BALB/c mice
413 in combination with aluminum hydroxide (Alum), Alum plus CpG7909, or Freund's adjuvant
414 (FA). As shown in Fig. 2A, the sE2-specific antibody titers of all mice from the three vaccine
415 groups peaked at week 6 and gradually decreased, but remained above 1,000, until week 22.
416 Following a homologous boost at week 25, a drastic increase in sE2-specific antibody titers
417 was observed at week 27 for the three vaccine groups but not the control group (Fig. 2A),
418 indicating the presence of sE2-specific B cell memory. Among the three experimental
419 vaccines, sE2 adjuvanted with FA, which is not approved for human use, elicited the highest
420 antibody titers at week 6 (Fig. 2B). The sE2-specific antibody titers of the sE2/Alum/CpG7909

group were significantly higher than those of the sE2/Alum group (Fig. 2B). Moreover, the sE2/Alum group predominantly produced the IgG1 subclass of antibodies (Fig. 2C), confirming that Alum is a T helper (Th) 2-biased adjuvant. The addition of CpG7909 resulted in a low IgG1/IgG2a ratio (Fig. 2C), indicating that CpG re-directs the Th cell bias from Th2 to Th1.

Antigen-specific T cell responses induced by the immunizations were assessed by ELISPOT in splenocytes. The three vaccine groups, but not the control, showed significantly higher numbers of IFN-γ- and interleukin (IL)-4-secreting cells (Fig. 2D). Therefore, immunization of mice with sE2 can elicit antigen-specific IFN-γ- and IL-4-T cell memory, which can be rapidly recalled to respond to subsequent viral antigen exposure.

The ability of the mouse antisera to inhibit HCV infection *in vitro* was assessed by a micro-neutralization assay using a panel of chimeric HCVcc containing envelope proteins of 12 different strains, which cover nine sub-genotypes in all the seven genotypes (30-33). As shown in Fig. 3A, anti-sE2 sera at a 1:40 dilution were able to efficiently neutralize (neutralization ≥50%) almost all of the HCVcc in the panel. Antisera from a minority of the mice had relatively poor neutralization (neutralization＜50%) against only J6 and QC69. Notably, PR52B6mt and PR79L9, containing envelope proteins constructed directly from two clinical isolates (33), were effectively neutralized. As shown in Table 1, for the three sE2 vaccine groups, the pooled sera titers that yielded ≥50% neutralization (NT_{50}) were no less than 40 against all the HCVcc tested. Among them, the sE2/Alum/CpG antisera appeared to be the most effective in terms of overall neutralization potency and breadth, with NT_{50}≥160 for all the HCVcc strains.

443 The above data demonstrate that sE2 can elicit the production of bNAbs. To determine
444 whether the induced bNAbs target different neutralizing epitopes, we developed a competitive
445 ELISA, in which HRP-conjugated AP33 and AR3A were used as the detection antibodies. The
446 results from competitive ELISAs showed that sE2 binding to both AP33 and AP3A was
447 inhibited by pre-incubation with the antisera from the three sE2 vaccine groups in a
448 dose-dependent manner, whereas the control sera from the PBS group did not exhibit
449 significant inhibitory effects (Fig. 3B). These data indicate the presence of both AP33-like and
450 AR3A-like broadly neutralizing antibodies in the anti-sE2 sera, which may contribute to the
451 observed broad neutralization by the anti-sE2 sera.
452
453 **Oligomeric state of sE2 does not affect bNAb induction**
454 A previous study showed that a similar version of sE2 produced in mammalian cells
455 existed primarily in monomeric and dimeric forms (40). To define the oligomeric state of our
456 insect cell-produced sE2, we subjected the Ni-NTA-purified sE2 to SEC analysis. Three major
457 peaks were identified in the SEC chromatogram (Fig. 4A). Non-reducing SDS-PAGE showed
458 that monomers (~45kDa) and dimers (~90kDa) were predominantly detected in the peak 3
459 and the peak 2, respectively, whereas the peak 1 contained large-molecular-mass protein
460 probably representing sE2 megamers (Fig. 4B). To investigate the impact of sE2 oligomeric
461 state on bNAb induction, we immunized three groups of BALB/c mice with equal amount (50
462 ug) of sE2 antigens concentrated from the three peaks, respectively, and compared the
463 resulting mouse antisera for neutralization against different HCVcc genotypes. As shown in
464 Fig. 4C, despite that the antisera from mice immunized with the peak 3 antigen exhibited

decreased neutralization activity against the homologous strain Con1 as compared to the antisera from the other two groups (peak 1 and peak 2), no significant difference in neutralization against all of the heterologous strains tested was observed for the three sE2 vaccine groups. These results indicate that oligomeric state of sE2 does not affect its ability to induce bNAbs..

The unique glycosylation of insect cell-derived sE2 is critical for its ability to induce broadly neutralizing antibodies

Next, we analyzed the contribution of glycosylation on the induction of bNAbs by directly comparing the immunogenicity of sE2 produced in human HEK293T cells (Figs. 5A-B) with sE2 produced in Drosophila S2. Upon PNGase F treatment, both proteins yielded the same ~34kDa band (Figs. 5A and 5C); however, Endo H-treated mammalian sE2 showed a smeared (from 70kDa to 35kDa) banding pattern (Fig. 5A), which differs from that of Endo H-treated insect sE2 (Fig. 1D). These results demonstrate that the glycosylation patterns of insect and mammalian HCV sE2 are different, which is in line with previous studies comparing the envelope proteins of other viruses, e.g. influenza A virus, expressed in cells of heterologous species (42). Then, insect sE2 and mammalian sE2 were compared for mAb recognition. Both sE2 versions reacted with the AP33 mAb in an identical fashion, whereas mammalian sE2 was poorly recognized by the mAb AR3A as compared to insect sE2 (Fig. 5D); however, after PNGase F digestion to remove N-linked glycans (Fig. 5C), both deglycosylated sE2 proteins reacted equally with AR3A and AP33 antibodies (Fig. 5E). These antibody binding data indicate that glycosylation can affect epitope exposure on sE2.

Moreover, mammalian sE2 bound CD81 and SRB1 less efficiently than insect sE2 did, whereas their deglycosylated forms performed equally (Fig. 5F), although both sE2 versions compete with CD81LEL (Fig. 5G-H) and HCVcc (Fig. 5I). These results suggest that the better receptor recognition by insect sE2 is due to its unique glycosylation pattern.

To assess the impact of glycosylation on sE2's immunogenicity and NAb-inducing ability, we immunized four groups of BALB/c mice with insect sE2, mammalian sE2, or their N-linked deglycosylated counterparts. Among the four groups, the one immunized with insect sE2 produced the highest binding antibody titers (Fig. 5J) as well as the highest neutralization antibody titers against all HCVcc tested (Fig. 5K). Specifically, antisera induced by insect sE2 showed NT_{50}≥160 against all the tested HCVcc strains, whereas antisera of the mammalian sE2 group exhibited NT_{50}≥160 for only two strains (Con1 and JFH1) (Fig. 5K). In addition, removal of N-glycans from insect sE2 resulted in reduced sE2-binding and neutralization antibody titers (Fig. 5K). These data suggest that the unique glycosylation in insect cell-derived sE2 is critical for its ability to induce pan-genotypic neutralizing antibodies.

HVR1-deleted mutant is equivalent to the intact sE2 in eliciting bNAbs

Hypervariable region 1 (HVR1) is a highly variant region in the N-terminus of E2 and is a predominant neutralizing epitope in the context of natural infection. However, anti-HVR1 NAbs are mostly isolate-specific (18, 46), and HVR1 has been shown to play a detrimental role in virus neutralization (47-49). We therefore evaluated whether the deletion of HVR1 from sE2 (sE2ΔHVR1, Fig. 6A) would affect its conformation and ability to induce cross-reactive NAbs. sE2ΔHVR1 retained the ability to bind CD81, but poorly bound SRB1 (Fig. 6B), indicating that

509 HVR1 is involved in interacting with SRB1, in agreement with previous findings (50). The
510 ability of sE2ΔHVR1 to inhibit HCVcc infection was significantly impaired compared to
511 full-length sE2 (Fig. 6C), likely due to the failure of sE2ΔHVR1 to block the interaction
512 between HCVcc and SRB1. Both sE2ΔHVR1 and full-length sE2 were examined for their
513 ability to react with mAbs AR3A and AP33. As shown in Fig. 6D, the reactivity of sE2ΔHVR1 to
514 AR3A was nearly identical to that of full-length sE2, whereas binding of sE2ΔHVR1 to AP33
515 was much greater than full-length sE2, suggesting that HVR1 (aa. 384-410), present on
516 full-length sE2, somewhat masks the adjacent AP33 epitope (aa. 412-423).
517 Next, we immunized BALB/c mice with sE2 and sE2ΔHVR1. The sE2- and sE2ΔHVR1-
518 binding activities of antisera from both groups were similar (Fig. 6E). Although the neutralizing
519 ability of the anti-sE2ΔHVR1 sera against the homologous Con1 strain was significantly
520 impaired as compared to that of full-length sE2, no significant difference in neutralization of
521 the 11 heterologous strains was observed between the two antisera (Fig. 6F). These results
522 demonstrate that sE2ΔHVR1 is equivalent to the full-length sE2 in inducing broadly
523 neutralizing antibodies.
524
525 **Prophylactic efficacy of sE2 vaccine in a genetically humanized mouse model of HCV**
526 **infection**
527 The *in vivo* protective efficacy of the sE2 vaccine was evaluated using a genetically
528 humanized mouse model (12). Rosa26-Fluc mice immunized with sE2/Alum generated
529 high-titer sE2-specific antibodies whereas those injected with PBS/Alum did not (Fig. 7A-B,
530 *n*=6 per group). Following injection of adenoviruses expressing HCV entry factors (EF) CD81

and OCLN, the immunized Rosa26-Fluc mice were subsequently challenged with Jc1-derived bicistronic HCV encoding Cre recombinase (BiCre-Jc1, genotype 2a) (12). As shown in Fig. 7C-D, the bioluminescence signals were drastically reduced in the sE2/Alum immunized mice as compared to the PBS/Alum and the "no EF" groups. These results indicate that active immunization with sE2 can efficiently protect against HCV infection *in vivo.*

Discussion

Glycosylated envelope proteins of viruses are often the targets for vaccine development. Thus far, the role of glycosylation in vaccine immunogenicity remains controversial (51-54). Structural analysis suggested that N-linked glycans in HCV E2 mask the exposed face on the E2 surface from NAbs (55, 56). In the present study, we aimed to analyze the impact of glycosylation on the immunogenicity of a HCV E2 protein-based recombinant vaccine candidate. We demonstrate that the glycosylation pattern associated with S2 cell-derived sE2 may be more favorable to eliciting bNAbs than mammalian cell-produced sE2 (40). In our study, we show that the removal of N-glycans in sE2 markedly reduced the antibody titers (Fig. 5J). In addition, S2 cell-produced sE2, which is decorated with less complex glycans, not only was more immunogenic (Fig. 5J) but also had more exposed neutralizing epitopes (Fig. 5B-E) and receptor-binding domains (Fig. 5F) as compared to its mammalian cell-derived counterpart. This suggests that the unique glycosylation of S2 cell-produced sE2 is important for its bNAbs-inducing ability.

In addition to the altered glycosylation of insect cell derived sE2, we reason that increased conformational flexibility contributes to the greater immunogenicity we observed.

553 sE2 expressed in S2 cells appears to have acquired a critical conformation suitable for
554 inducing bNAbs, and such a conformation may not readily occur when E2 is presented in a
555 more complex structure, such as a virion or E1/E2 heterodimer. For example, HVR1 present
556 on HCV particles has been shown to obstruct the CD81 binding site, thereby masking
557 conserved neutralizing epitopes (50), and an initial contact with SRB1 may be needed to
558 unmask the binding site for E2 to interact with CD81. In addition, it has also been reported that
559 deletion of HVR1 enhances the CD81 binding activity of E1/E2 heterodimers in HCV
560 pseudo-particles (57). In contrast, we found that the deletion of HVR1 did not significantly
561 affect the CD81-binding activity of sE2 (Fig. 6B), indicating that the HVR1 domain in the
562 context of insect cell-produced sE2 does not functionally mask the CD81 binding site and
563 therefore may facilitate the elicitation of CD81 binding site-specific antibodies. In support of
564 this notion, structural studies suggest that in sE2, the region from HVR1 (residue 384-410) to
565 a conserved epitope (residue 412-423) is conformationally flexible (58, 59), which may aid in
566 exposure of the conserved epitope. Conceivably, this flexibility enables sE2 to represent
567 critical E2 intermediate form(s) in a transition-phase of HCV entry and may therefore be key to
568 the ability of sE2 to induce pan-genotypic NAbs.

569 Another important consideration for prioritizing HCV vaccine candidates is scalabilty for
570 potential mass production. Although the yields of insect and mammalian sE2s may differ for
571 other HCV strains, in this study, correctly folded sE2 of Con1 strain can be produced at high
572 levels in the S2 expression system (100 mg/L), which is considerably higher than the yields
573 (1-2 mg/L) of mammalian sE2 or a similar version termed eE2 (40). The yield could potentially

be further improved by using a perfusion culture technology as described previously (60). The identification of such a production system will be important for practical scaling up.

Thus far, only a few NAb-based vaccines have been evaluated *in vivo* due to the scarcity of small animal models for HCV infection (12, 19, 20, 23). For example, an inactivated HCV vaccine was found to induce NAbs capable of protecting chimeric uPA/SCID mice from lower doses (10^3 RNA copies of HCVcc) of HCV challenge, but not higher doses (10^4 and 10^5) (23). In this study, we used immunocompetent mice to assess the immunogenicity as well as prophylactic efficacy of the vaccine candidate. Proof-of-concept for the utility of this genetically humanized mouse model to test antibody-based vaccine candidates was previously established with a recombinant vaccinia-virus vector expressing the structural proteins of a genotype 1a HCV vaccine strain. Here, we employed this model to assess the efficacy of our recombinant vaccine candidate. We found that genetically humanized mice immunized with Con1 (genotype 1b)-derived sE2 were protected from heterologous challenge with 2×10^7 $TCID_{50}$ of BiCre-Jc1 (genotype 2a) HCVcc. As BiCre-Jc1 HCVcc is a relatively difficult-to-neutralize strain (Fig. 3A, and references(10-13)), the observed cross-protection highlights the potential of sE2 as a broadly protective HCV vaccine. While evaluation of the efficacy of this vaccine in chimpanzees – the only other known species to be readily susceptible to HCV infection – would be desirable, experimentation in great apes is banned in most countries and/or is no longer supported by federal funding due to ethical concerns. Thus, the genetically humanized mouse model remains to date the only immunocompetent animal model available to test preclinically the efficacy of vaccine candidates. We should point out that this mouse model is not without caveats. For example, since not all of the identified

596 human receptors/co-factors for HCV (17) are present in this model, it may be easier to prevent
597 infection in this model than with natural infection. Nevertheless, we have previously shown
598 that levels of protection correlate well with the immunogenicity of vectored vaccines in this
599 model (12) and thus such humanized mice seem adequate for evaluating the efficacy of our
600 recombinant HCV vaccine.
601
602 In conclusion, a sE2 vaccine based on expression of viral envelope proteins in insect
603 cells has multiple benefits. Firstly, the simple glycosylation and high flexibility of insect
604 cell-derived sE2 may aid its ability to induce bNAbs, as demonstrated by the highly broad
605 NAbs observed in mice. Secondly, industrial production-related advantages, such as simple
606 composition, high yield, and ease in purification, will greatly reduce production costs and also
607 make it possible to develop a multivalent vaccine formulation for broader coverage if needed.
608 Thirdly, the *in vivo* protective efficacy of sE2 was confirmed by an active immunization,
609 instead of a passive immunization, in a humanized mouse model, which is the only
610 immunocompetent animal model (except chimpanzee) of HCV infection currently available.
611 These results should encourage further pre-clinical and clinical development of a sE2-based,
612 broadly protective HCV vaccine.
613
614
615
616 **References**

1. **El-Serag, H. B.** 2012. Epidemiology of viral hepatitis and hepatocellular carcinoma. Gastroenterology **142:**1264-1273 e1261.

2. **Gonzalez-Grande, R., M. Jimenez-Perez, C. Gonzalez Arjona, and J. Mostazo Torres.** 2016. New approaches in the treatment of hepatitis C. World journal of gastroenterology **22:**1421-1432.

3. **Barnes, E., A. Folgori, S. Capone, L. Swadling, S. Aston, A. Kurioka, J. Meyer, R. Huddart, K. Smith, R. Townsend, A. Brown, R. Antrobus, V. Ammendola, M. Naddeo, G. O'Hara, C. Willberg, A. Harrison, F. Grazioli, M. L. Esposito, L. Siani, C. Traboni, Y. Oo, D. Adams, A. Hill, S. Colloca, A. Nicosia, R. Cortese, and P. Klenerman.** 2012. Novel adenovirus-based vaccines induce broad and sustained T cell responses to HCV in man. Science translational medicine **4:**115ra111.

4. **Swadling, L., S. Capone, R. D. Antrobus, A. Brown, R. Richardson, E. W. Newell, J. Halliday, C. Kelly, D. Bowen, J. Fergusson, A. Kurioka, V. Ammendola, M. Del Sorbo, F. Grazioli, M. L. Esposito, L. Siani, C. Traboni, A. Hill, S. Colloca, M. Davis, A. Nicosia, R. Cortese, A. Folgori, P. Klenerman, and E. Barnes.** 2014. A human vaccine strategy based on chimpanzee adenoviral and MVA vectors that primes, boosts, and sustains functional HCV-specific T cell memory. Science translational medicine **6:**261ra153.

5. **Burton, D. R., P. Poignard, R. L. Stanfield, and I. A. Wilson.** 2012. Broadly neutralizing antibodies present new prospects to counter highly antigenically diverse viruses. Science **337:**183-186.

6. **Pestka, J. M., M. B. Zeisel, E. Bläser, P. Schürmann, B. Bartosch, F.-L. L. Cosset, A. H. Patel, H. Meisel, J. Baumert, S. Viazov, K. Rispeter, H. E. Blum, M. Roggendorf, and**

639 **T. F. Baumert.** 2007. Rapid induction of virus-neutralizing antibodies and viral clearance in a
640 single-source outbreak of hepatitis C. Proceedings of the National Academy of Sciences of
641 the United States of America **104:**6025-6030.
642 7. **Lavillette, D., Y. Morice, G. Germanidis, P. Donot, A. Soulier, E. Pagkalos, G.**
643 **Sakellariou, L. Intrator, B. Bartosch, J. M. Pawlotsky, and F. L. Cosset.** 2005. Human
644 serum facilitates hepatitis C virus infection, and neutralizing responses inversely correlate
645 with viral replication kinetics at the acute phase of hepatitis C virus infection. J Virol
646 **79:**6023-6034.
647 8. **Dowd, K. A., D. M. Netski, X. H. Wang, A. L. Cox, and S. C. Ray.** 2009. Selection
648 pressure from neutralizing antibodies drives sequence evolution during acute infection with
649 hepatitis C virus. Gastroenterology **136:**2377-2386.
650 9. **Morin, T. J., T. J. Broering, B. A. Leav, B. M. Blair, K. J. Rowley, E. N. Boucher, Y.**
651 **Wang, P. S. Cheslock, M. Knauber, D. B. Olsen, S. W. Ludmerer, G. Szabo, R. W.**
652 **Finberg, R. H. Purcell, R. E. Lanford, D. M. Ambrosino, D. C. Molrine, and G. J. Babcock.**
653 2012. Human monoclonal antibody HCV1 effectively prevents and treats HCV infection in
654 chimpanzees. PLoS pathogens **8:**e1002895.
655 10. **Law, M., T. Maruyama, J. Lewis, E. Giang, A. Tarr, Z. Stamataki, P. Gastaminza, F.**
656 **Chisari, I. Jones, R. Fox, J. Ball, J. McKeating, N. Kneteman, and D. Burton.** 2008.
657 Broadly neutralizing antibodies protect against hepatitis C virus quasispecies challenge.
658 Nature medicine **14:**25-27.
659 11. **Giang, E., M. Dorner, J. C. Prentoe, M. Dreux, M. J. Evans, J. Bukh, C. M. Rice, A.**
660 **Ploss, D. R. Burton, and M. Law.** 2012. Human broadly neutralizing antibodies to the

envelope glycoprotein complex of hepatitis C virus. Proceedings of the National Academy of Sciences of the United States of America **109:**6205-6210.

12. **Dorner, M., J. A. Horwitz, J. B. Robbins, W. T. Barry, Q. Feng, K. Mu, C. T. Jones, J. W. Schoggins, M. T. Catanese, D. R. Burton, M. Law, C. M. Rice, and A. Ploss.** 2011. A genetically humanized mouse model for hepatitis C virus infection. Nature **474:**208-211.

13. **de Jong, Y. P., M. Dorner, M. C. Mommersteeg, J. W. Xiao, A. B. Balazs, J. B. Robbins, B. Y. Winer, S. Gerges, K. Vega, R. N. Labitt, B. M. Donovan, E. Giang, A. Krishnan, L. Chiriboga, M. R. Charlton, D. R. Burton, D. Baltimore, M. Law, C. M. Rice, and A. Ploss.** 2014. Broadly neutralizing antibodies abrogate established hepatitis C virus infection. Science translational medicine **6:**254ra129.

14. **Desombere, I., S. Fafi-Kremer, F. Van Houtte, P. Pessaux, A. Farhoudi, L. Heydmann, L. Verhoye, S. Cole, J. A. McKeating, G. Leroux-Roels, T. F. Baumert, A. H. Patel, and P. Meuleman.** 2016. Monoclonal anti-envelope antibody AP33 protects humanized mice against a patient-derived hepatitis C virus challenge. Hepatology **63:**1120-1134.

15. **Prince, A. M., B. Brotman, D. H. Lee, W. Pfahler, N. Tricoche, L. Andrus, and M. T. Shata.** 2005. Protection against chronic hepatitis C virus infection after rechallenge with homologous, but not heterologous, genotypes in a chimpanzee model. The Journal of infectious diseases **192:**1701-1709.

16. **Lindenbach, B., and C. Rice.** 2013. The ins and outs of hepatitis C virus entry and assembly. Nature reviews. Microbiology **11:**688-700.

17. **Ding, Q., M. von Schaewen, and A. Ploss.** 2014. The impact of hepatitis C virus entry on viral tropism. Cell host & microbe **16:**562-568.

18. **Wang, Y., Z.-Y. Keck, and S. Foung.** 2011. Neutralizing antibody response to hepatitis C virus. Viruses **3:**2127-2145.

19. **Choo, Q. L., G. Kuo, R. Ralston, A. Weiner, D. Chien, G. Van Nest, J. Han, K. Berger, K. Thudium, C. Kuo, J. Kansopon, J. McFarland, A. Tabrizi, K. Ching, B. Moss, L. B. Cummins, M. Houghton, and E. Muchmore.** 1994. Vaccination of chimpanzees against infection by the hepatitis C virus. Proceedings of the National Academy of Sciences of the United States of America **91:**1294-1298.

20. **Elmowalid, G. A., M. Qiao, S. H. Jeong, B. B. Borg, T. F. Baumert, R. K. Sapp, Z. Hu, K. Murthy, and T. J. Liang.** 2007. Immunization with hepatitis C virus-like particles results in control of hepatitis C virus infection in chimpanzees. Proceedings of the National Academy of Sciences of the United States of America **104:**8427-8432.

21. **Garrone, P., A.-C. Fluckiger, P. Mangeot, E. Gauthier, P. Dupeyrot-Lacas, J. Mancip, A. Cangialosi, I. Du Chéné, R. LeGrand, I. Mangeot, D. Lavillette, B. Bellier, F.-L. Cosset, F. Tangy, D. Klatzmann, and C. Dalba.** 2011. A prime-boost strategy using virus-like particles pseudotyped for HCV proteins triggers broadly neutralizing antibodies in macaques. Science translational medicine **3**.

22. **Reyes-del Valle, J., C. de la Fuente, M. Turner, C. Springfeld, S. Apte-Sengupta, M. Frenzke, A. Forest, J. Whidby, J. Marcotrigiano, C. Rice, and R. Cattaneo.** 2012. Broadly neutralizing immune responses against hepatitis C virus induced by vectored measles viruses and a recombinant envelope protein booster. Journal of virology **86:**11558-11566.

704 23. **Akazawa, D., M. Moriyama, H. Yokokawa, N. Omi, N. Watanabe, T. Date, K.**
705 **Morikawa, H. Aizaki, K. Ishii, T. Kato, H. Mochizuki, N. Nakamura, and T. Wakita.** 2013.
706 Neutralizing antibodies induced by cell culture-derived hepatitis C virus protect against
707 infection in mice. Gastroenterology **145:**447-455 e441-444.
708 24. **Beaumont, E., R. Patient, C. Hourioux, I. Dimier-Poisson, and P. Roingeard.** 2013.
709 Chimeric hepatitis B virus/hepatitis C virus envelope proteins elicit broadly neutralizing
710 antibodies and constitute a potential bivalent prophylactic vaccine. Hepatology (Baltimore,
711 Md.) **57:**1303-1313.
712 25. **Law, J., C. Chen, J. Wong, D. Hockman, D. Santer, S. Frey, R. Belshe, T. Wakita, J.**
713 **Bukh, C. Jones, C. Rice, S. Abrignani, D. Tyrrell, and M. Houghton.** 2013. A hepatitis C
714 virus (HCV) vaccine comprising envelope glycoproteins gpE1/gpE2 derived from a single
715 isolate elicits broad cross-genotype neutralizing antibodies in humans. PloS one **8**.
716 26. **Chmielewska, A. M., M. Naddeo, S. Capone, V. Ammendola, K. Hu, L. Meredith, L.**
717 **Verhoye, M. Rychlowska, R. Rappuoli, J. B. Ulmer, S. Colloca, A. Nicosia, R. Cortese, G.**
718 **Leroux-Roels, P. Balfe, K. Bienkowska-Szewczyk, P. Meuleman, J. A. McKeating, and A.**
719 **Folgori.** 2014. Combined adenovirus vector and hepatitis C virus envelope protein
720 prime-boost regimen elicits T cell and neutralizing antibody immune responses. Journal of
721 virology **88:**5502-5510.
722 27. **Stamataki, Z., S. Coates, M. J. Evans, M. Wininger, K. Crawford, C. Dong, Y. L.**
723 **Fong, D. Chien, S. Abrignani, P. Balfe, C. M. Rice, J. A. McKeating, and M. Houghton.**
724 2007. Hepatitis C virus envelope glycoprotein immunization of rodents elicits cross-reactive
725 neutralizing antibodies. Vaccine **25:**7773-7784.

28. **Frey, S. E., M. Houghton, S. Coates, S. Abrignani, D. Chien, D. Rosa, P. Pileri, R. Ray, A. M. Di Bisceglie, P. Rinella, H. Hill, M. C. Wolff, V. Schultze, J. H. Han, B. Scharschmidt, and R. B. Belshe.** 2010. Safety and immunogenicity of HCV E1E2 vaccine adjuvanted with MF59 administered to healthy adults. Vaccine **28:**6367-6373.

29. **Lindenbach, B. D., P. Meuleman, A. Ploss, T. Vanwolleghem, A. J. Syder, J. A. McKeating, R. E. Lanford, S. M. Feinstone, M. E. Major, G. Leroux-Roels, and C. M. Rice.** 2006. Cell culture-grown hepatitis C virus is infectious in vivo and can be recultured in vitro. Proceedings of the National Academy of Sciences of the United States of America **103:**3805-3809.

30. **Zhong, J., P. Gastaminza, G. Cheng, S. Kapadia, T. Kato, D. R. Burton, S. F. Wieland, S. L. Uprichard, T. Wakita, and F. V. Chisari.** 2005. Robust hepatitis C virus infection in vitro. Proceedings of the National Academy of Sciences of the United States of America **102:**9294-9299.

31. **Pietschmann, T., A. Kaul, G. Koutsoudakis, A. Shavinskaya, S. Kallis, E. Steinmann, K. Abid, F. Negro, M. Dreux, F. L. Cosset, and R. Bartenschlager.** 2006. Construction and characterization of infectious intragenotypic and intergenotypic hepatitis C virus chimeras. Proceedings of the National Academy of Sciences of the United States of America **103:**7408-7413.

32. **Gottwein, J., T. Scheel, T. Jensen, J. Lademann, J. Prentoe, M. Knudsen, A. Hoegh, and J. Bukh.** 2009. Development and characterization of hepatitis C virus genotype 1-7 cell culture systems: role of CD81 and scavenger receptor class B type I and effect of antiviral drugs. Hepatology (Baltimore, Md.) **49:**364-377.

748 33. **Lu, J., W. Tao, R. Li, Y. Xiang, N. Zhang, X. Xiang, Q. Xie, and J. Zhong.** 2013.
749 Construction and characterization of infectious hepatitis C virus chimera containing structural
750 proteins directly from genotype 1b clinical isolates. Virology **443:**80-88.
751 34. **Tao, W., C. Xu, Q. Ding, R. Li, Y. Xiang, J. Chung, and J. Zhong.** 2009. A single point
752 mutation in E2 enhances hepatitis C virus infectivity and alters lipoprotein association of viral
753 particles. Virology **395:**67-76.
754 35. **Owsianka, A., A. W. Tarr, V. S. Juttla, D. Lavillette, B. Bartosch, F. L. Cosset, J. K.**
755 **Ball, and A. H. Patel.** 2005. Monoclonal antibody AP33 defines a broadly neutralizing epitope
756 on the hepatitis C virus E2 envelope glycoprotein. Journal of virology **79:**11095-11104.
757 36. **Li, R., Y. Qin, Y. He, W. Tao, N. Zhang, C. Tsai, P. Zhou, and J. Zhong.** 2011.
758 Production of hepatitis C virus lacking the envelope-encoding genes for single-cycle infection
759 by providing homologous envelope proteins or vesicular stomatitis virus glycoproteins in
760 trans. Journal of virology **85:**2138-2147.
761 37. **Lindenbach, B. D., M. J. Evans, A. J. Syder, B. Wolk, T. L. Tellinghuisen, C. C. Liu,**
762 **T. Maruyama, R. O. Hynes, D. R. Burton, J. A. McKeating, and C. M. Rice.** 2005.
763 Complete replication of hepatitis C virus in cell culture. Science **309:**623-626.
764 38. **Naarding, M. A., E. Falkowska, H. Xiao, and T. Dragic.** 2011. Hepatitis C virus soluble
765 E2 in combination with QuilA and CpG ODN induces neutralizing antibodies in mice. Vaccine
766 **29:**2910-2917.
767 39. **Ruwona, T. B., E. Giang, T. Nieusma, and M. Law.** 2014. Fine mapping of murine
768 antibody responses to immunization with a novel soluble form of hepatitis C virus envelope
769 glycoprotein complex. J Virol **88:**10459-10471.

40. **Whidby, J., G. Mateu, H. Scarborough, B. Demeler, A. Grakoui, and J. Marcotrigiano.** 2009. Blocking hepatitis C virus infection with recombinant form of envelope protein 2 ectodomain. Journal of virology **83:**11078-11089.

41. **Helle, F., G. Duverlie, and J. Dubuisson.** 2011. The hepatitis C virus glycan shield and evasion of the humoral immune response. Viruses **3:**1909-1932.

42. **de Vries, R. P., C. H. Smit, E. de Bruin, A. Rigter, E. de Vries, L. A. Cornelissen, D. Eggink, N. P. Chung, J. P. Moore, R. W. Sanders, C. H. Hokke, M. Koopmans, P. J. Rottier, and C. A. de Haan.** 2012. Glycan-dependent immunogenicity of recombinant soluble trimeric hemagglutinin. Journal of virology **86:**11735-11744.

43. **Yang, L., Y. Song, X. Li, X. Huang, J. Liu, H. Ding, P. Zhu, and P. Zhou.** 2012. HIV-1 virus-like particles produced by stably transfected Drosophila S2 cells: a desirable vaccine component. Journal of virology **86:**7662-7676.

44. **Scarselli, E., H. Ansuini, R. Cerino, R. M. Roccasecca, S. Acali, G. Filocamo, C. Traboni, A. Nicosia, R. Cortese, and A. Vitelli.** 2002. The human scavenger receptor class B type I is a novel candidate receptor for the hepatitis C virus. EMBO J **21:**5017-5025.

45. **Pileri, P., Y. Uematsu, S. Campagnoli, G. Galli, F. Falugi, R. Petracca, A. J. Weiner, M. Houghton, D. Rosa, G. Grandi, and S. Abrignani.** 1998. Binding of hepatitis C virus to CD81. Science **282:**938-941.

46. **Edwards, V. C., A. W. Tarr, R. A. Urbanowicz, and J. K. Ball.** 2012. The role of neutralizing antibodies in hepatitis C virus infection. The Journal of general virology **93:**1-19.

790 47. **Prentoe, J., L. Verhoye, R. Velazquez Moctezuma, C. Buysschaert, A. Farhoudi, R.**
791 **Wang, H. Alter, P. Meuleman, and J. Bukh.** 2015. HVR1-mediated antibody evasion of
792 highly infectious in vivo adapted HCV in humanised mice. Gut.
793 48. **Prentoe, J., T. B. Jensen, P. Meuleman, S. B. Serre, T. K. Scheel, G. Leroux-Roels,**
794 **J. M. Gottwein, and J. Bukh.** 2011. Hypervariable region 1 differentially impacts viability of
795 hepatitis C virus strains of genotypes 1 to 6 and impairs virus neutralization. Journal of
796 virology **85:**2224-2234.
797 49. **Bankwitz, D., E. Steinmann, J. Bitzegeio, S. Ciesek, M. Friesland, E. Herrmann, M.**
798 **B. Zeisel, T. F. Baumert, Z. Y. Keck, S. K. Foung, E. I. Pecheur, and T. Pietschmann.**
799 2010. Hepatitis C virus hypervariable region 1 modulates receptor interactions, conceals the
800 CD81 binding site, and protects conserved neutralizing epitopes. Journal of virology
801 **84:**5751-5763.
802 50. **Bankwitz, D., E. Steinmann, J. Bitzegeio, S. Ciesek, M. Friesland, E. Herrmann, M.**
803 **Zeisel, T. Baumert, Z.-y. Keck, S. Foung, E.-I. Pécheur, and T. Pietschmann.** 2010.
804 Hepatitis C virus hypervariable region 1 modulates receptor interactions, conceals the CD81
805 binding site, and protects conserved neutralizing epitopes. Journal of virology **84:**5751-5763.
806 51. **Ma, B. J., S. M. Alam, E. P. Go, X. Lu, H. Desaire, G. D. Tomaras, C. Bowman, L. L.**
807 **Sutherland, R. M. Scearce, S. Santra, N. L. Letvin, T. B. Kepler, H. X. Liao, and B. F.**
808 **Haynes.** 2011. Envelope deglycosylation enhances antigenicity of HIV-1 gp41 epitopes for
809 both broad neutralizing antibodies and their unmutated ancestor antibodies. PLoS pathogens
810 **7:**e1002200.

811 52. **Banerjee, K., S. Andjelic, P. J. Klasse, Y. Kang, R. W. Sanders, E. Michael, R. J.**
812 **Durso, T. J. Ketas, W. C. Olson, and J. P. Moore.** 2009. Enzymatic removal of mannose
813 moieties can increase the immune response to HIV-1 gp120 in vivo. Virology **389:**108-121.
814 53. **Gavrilov, B. K., K. Rogers, I. J. Fernandez-Sainz, L. G. Holinka, M. V. Borca, and G.**
815 **R. Risatti.** 2011. Effects of glycosylation on antigenicity and immunogenicity of classical
816 swine fever virus envelope proteins. Virology **420:**135-145.
817 54. **Hutter, J., J. V. Rodig, D. Hoper, P. H. Seeberger, U. Reichl, E. Rapp, and B.**
818 **Lepenies.** 2013. Toward animal cell culture-based influenza vaccine design: viral
819 hemagglutinin N-glycosylation markedly impacts immunogenicity. Journal of immunology
820 **190:**220-230.
821 55. **Khan, A. G., J. Whidby, M. T. Miller, H. Scarborough, A. V. Zatorski, A. Cygan, A. A.**
822 **Price, S. A. Yost, C. D. Bohannon, J. Jacob, A. Grakoui, and J. Marcotrigiano.** 2014.
823 Structure of the core ectodomain of the hepatitis C virus envelope glycoprotein 2. Nature
824 **509:**381-384.
825 56. **Kong, L., E. Giang, T. Nieusma, R. U. Kadam, K. E. Cogburn, Y. Hua, X. Dai, R. L.**
826 **Stanfield, D. R. Burton, A. B. Ward, I. A. Wilson, and M. Law.** 2013. Hepatitis C virus E2
827 envelope glycoprotein core structure. Science **342:**1090-1094.
828 57. **Guan, M., W. Wang, X. Liu, Y. Tong, Y. Liu, H. Ren, S. Zhu, J. Dubuisson, T. F.**
829 **Baumert, Y. Zhu, H. Peng, L. Aurelian, P. Zhao, and Z. Qi.** 2012. Three different functional
830 microdomains in the hepatitis C virus hypervariable region 1 (HVR1) mediate entry and
831 immune evasion. The Journal of biological chemistry **287:**35631-35645.

58. **Meola, A., A. W. Tarr, P. England, L. W. Meredith, C. P. McClure, S. K. Foung, J. A. McKeating, J. K. Ball, F. A. Rey, and T. Krey.** 2015. Structural flexibility of a conserved antigenic region in hepatitis C virus glycoprotein E2 recognized by broadly neutralizing antibodies. Journal of virology **89:**2170-2181.

59. **Taniguchi, S., H. Okamoto, M. Sakamoto, M. Kojima, F. Tsuda, T. Tanaka, E. Munekata, E. E. Muchmore, D. A. Peterson, and S. Mishiro.** 1993. A structurally flexible and antigenically variable N-terminal domain of the hepatitis C virus E2/NS1 protein: implication for an escape from antibody. Virology **195:**297-301.

60. **Wang, L., H. Hu, J. Yang, F. Wang, C. Kaisermayer, and P. Zhou.** 2012. High yield of human monoclonal antibody produced by stably transfected Drosophila schneider 2 cells in perfusion culture using wave bioreactor. Mol Biotechnol **52:**170-179.

Acknowledgments: We thank Dr. Jens Bukh (University of Copenhagen) for providing chimeric HCVcc plasmids, Drs. Mansun Law and Dennis Burton (The Scripps Research Institute) for providing mAb AR3A, Dr. Arvind Patel (University of Glasgow) for providing mAb AP33 and Jenna Gaska for edits of the manuscript.

Funding: This work was supported in part by grants from the Chinese National Science and Technology Major Project (2012ZX10002007-003) (to J.Z. and Z.H.), the CAS/SAFEA International Partnership Program for Creative Research Teams (to J.Z.) and the National Institutes of Health (R01 AI079031-05, to A.P.) and a Research Scholar Grant, RSG-15-048-01 MPC from the American Cancer Society (to A.P.). A.P. is further supported

854 by the Investigators in the Pathogenesis of Infectious Disease (PATH) Award from the
855 Burroughs Wellcome Fund. M.v.S. is a recipient of a postdoctoral fellowship from the German
856 Research Foundation.

857 **Figure legends**

858 **FIG 1 Expression and characterization of sE2 derived from stably transfected**

859 ***Drosophila* S2 Cells.**

860 (A) The schematic diagrams of sE2 expression construct. Truncated E2 (aa. 384-661) gene

861 from the Con1 strain was inserted between the BiP signal peptide and the His-tag. (B)

862 Western blot analysis of sE2 accumulation in the supernatant of the stably transfected S2 cell

863 culture after different periods of induction. (C) SDS-PAGE analysis of purified sE2. (D)

864 Analysis of sE2 glycosylation by PNGase F or Endo H digestion. Glycosidase treated and

865 untreated samples were then subjected to Western blotting with anti-E2 (AP33) or anti-His

866 mAb as the detection antibody. (E) Receptor binding assay. sE2 protein was incubated with

867 wild-type CHO (CHO-WT), CHO-CD81, or CHO-SRB1 cells, stained with anti-His mAb

868 followed by Alexa Fluor-555 conjugated anti-mouse IgG, and detected by flow cytometry. (F)

869 Dose-dependently competitive inhibition of sE2 binding to CHO-CD81 cells by CD81LEL. sE2

870 was incubated with different doses of CD81LEL before performing the receptor-binding assay.

871 (G) Blockade of HCVcc infection by sE2. Serially diluted sE2 was mixed with HCVcc, and the

872 mixtures were added to Huh7.5.1 cells to allow infection for 4 h. CD81LEL and BSA were set

873 as controls. NS5A-immunostaining was performed at 72 h post-infection. Means ± SEM of the

874 triplicates are shown. (H) Recognition of sE2 by neutralizing mAbs AR3A (1 μg/mL) or AP33

875 (1 μg/mL). Means ± SEM of the OD450 readings from triplicate wells are shown.

876

877

878 **FIG 2 Induction of antibody and cellular-mediated immune responses in mice.**

879 (A) Kinetics of sE2-specific antibody titers. BALB/c (*n*=10 per group) mice were immunized
880 intraperitoneally at weeks 0, 2, 4, and 25 (arrowed), and the serum titers were measured by
881 ELISA. Data are expressed as the mean ± SEM of the endpoint titers for each group. (B)
882 Anti-sE2 IgG titers at week 6. (C) IgG1/IgG2a ratios of sE2 specific antibodies at week 6.
883 Horizontal lines indicate the geometric means for each group. Asterisks represent significant
884 differences between groups. Statistical significance was calculated by Kruskal-Wallis
885 One-Way ANOVA analysis. (D) Cellular immune responses as measured by IFN-γ and IL-4
886 ELISPOT assays. Splenocytes were isolated from mice spleens at week 27, pooled and
887 stimulated with sE2 protein. Results are expressed as spot-forming cells (SFCs) per 10^6
888 splenocytes. Means ± SEM of triplicate wells were shown. Asterisks represent significant
889 differences (two-tailed student *t* test) between medium (white bars) and sE2 stimulation (blue
890 bars) in each group. Ns (no significance), $P \geq 0.05$; *, $P < 0.05$; **, $P < 0.01$; ***, $P < 0.001$.

891

892 **FIG 3 Induction of bNAbs against HCVcc of genotypes 1-7 in mice.**

893 (A) Neutralization assay. Mouse antisera collected at week 27 were diluted 1:40 and then
894 tested for neutralization of a panel of HCVcc consisting of 12 strains from 7 genotypes. The
895 names of the indicated HCVcc were shown as “strain(genotype)” in each graph. Each symbol
896 represents one animal and the horizontal lines indicate the geometric means for each group.
897 The data are representative of three independent experiments. (B) Competitive ELISA.

898 Mouse antisera were serially diluted and tested for inhibition of AR3A and AP33 binding sE2.
899 Means ± SEM of the OD450 readings for all animals in each group are shown.

900

901 **FIG 4 Analysis of oligomeric states of sE2 and their bNAb-inducing ability.**

902 (A) Size exclusion chromatography of insect sE2 revealed three major peaks representing
903 different oligomeric states. (B) Analysis of the samples from the three peaks by SDS-PAGE
904 under non-reducing and reducing conditions. Megamers, tetramers (~170kDa), trimers
905 (~130kDa), dimers (~90kDa), and monomers (~45kDa) were indicated by arrows. (C)
906 Neutralization activities of the antisera. Four groups of mice were immunized with PBS, or one
907 of the antigens from the three peaks, respectively, and the resulting antisera were tested at
908 1:40 dilution for neutralization of a panel of HCVcc as indicated. Asterisks represent
909 significant differences (Kruskal-Wallis One-Way ANOVA) between groups: ns (no
910 significance); *, P<0.05; **, P<0.01.

911

912 **FIG 5 Comparative analyses of mammalian cell- and insect cell-derived sE2 proteins.**

913 (A) Western blot analysis of mammalian cell-derived sE2 without or with PNGase F or Endo H
914 digestion. (B) SDS-PAGE analysis of insect sE2 and mammalian sE2. (C) SDS-PAGE
915 analysis of PNGase F-treated insect sE2 and mammalian sE2. (D-E) Reactivity of different
916 sE2 forms with neutralizing mAbs AR3A (1 μg/mL) or AP33 (5 μg/mL) in ELISAs. Error bars
917 indicate Means ± SEM. Statistical significance was calculated by two-tailed student *t* test: ns
918 (no significance), P≥0.05; ***, P<0.001. Representative results of three independent

experiments are shown. (F) Binding of the glycosylated or N-deglycosylated mammalian and insect sE2 to CHO-WT, CHO-CD81, or CHO-SRB1 cells measured by flow cytometry. Representative results of three independent experiments are shown. (G-H) Competitive inhibition of insect sE2 (G) or mammalian sE2 (H) binding to CHO-CD81 cells by CD81LEL. (I) Comparison of HCVcc infection blocking by insect sE2 and mammalian sE2. Means ± SEM of the triplicates are shown. (J) sE2-specific antibody endpoint titers. Groups of mice (*n*=6 per group) were immunized with 40μg of mammalian sE2, insect sE2, N-deglycosylated mammalian sE2, or N-deglycosylated insect sE2, respectively, in the presence of 500μg Alum adjuvant. Another group was injected with PBS plus Alum, serving as the control. sE2-specific antibody endpoint titers were determined by ELISA. Each symbol represents one animal and the line indicates the geometric mean value of the group. Statistical significance was calculated by Kruskal-Wallis One-Way ANOVA analysis: *, $P<0.05$; ***, $P<0.001$. (K) NT_{50}s of the pooled antisera against a panel of HCVcc.

FIG 6 Effect of HVR1 in induction of broadly NAbs.

(A) SDS-PAGE analysis of purified sE2ΔHVR1 and full-length sE2. (B) Receptor binding functions of sE2ΔHVR1 and sE2 analyzed by flow cytometry. The deletion of HVR1 diminished sE2 binding to SRB1, while not affecting sE2 binding to CD81. Results shown are representative of three independent experiments. (C) Significantly weaker blockage of HCVcc infection by sE2ΔHVR1 comparing to sE2. Mean values ± SEM from three independent experiments performed in duplicate were shown. Asterisks represent significant differences (two-tailed student *t* test) between sE2 and sE2ΔHVR1 groups: ns (no significance), $P\geq0.05$;

941 *, *P*<0.05; **, *P*<0.01; ***, *P*<0.001. (D) Reactivity of sE2 and sE2ΔHVR1 to AR3A or AP33
942 mAbs. Serial diluted sE2, sE2ΔHVR1 or BSA samples were coated in ELISA plates and
943 detected by AR3A or AP33 mAb. Data are mean values ± SEM of triplicate wells. (E-F)
944 Comparison of neutralization activities of antisera induced by sE2 and that by sE2ΔHVR1.
945 BALB/c mice (*n*=6 per group) were injected intraperitoneally using sE2, sE2ΔHVR1 or PBS
946 (all adjuvanted by Alum) for four times. sE2-specific or sE2ΔHVR1-specific antibody titers of
947 mouse sera in each group were measured by ELISA. Mean values ± SEM of all animals in
948 each group were shown (E). Neutralization of the sE2- and the sE2ΔHVR1-immunized mouse
949 sera (1:40 diluted) against HCVcc of genotypes 1-7 were compared (F). Horizontal lines
950 indicate geometric means for each group. The results are representative of three independent
951 experiments.

952

953 **FIG 7 Prophylactic efficacy of active vaccination with sE2.**

954 ROSA26-Fluc mice were injected intraperitoneally at week 0, 1, 3 and 6 (green arrow) with 50
955 μg sE2 plus 1 ug Alum per mouse (*n*=6) or with PBS plus Alum (*n*=6). (A) Anti-sE2 endpoint
956 titers were measured by ELISA and plotted for the indicated time points. (B) Anti-sE2 IgG
957 titers for the day of challenge with HCVcc (red arrow, day 72 post first injection). Mean values
958 ± SD of all animals in each group were shown. (C) *In vivo* imaging for the HCVcc challenged
959 ROSA26-Fluc mice. At week 11, human HCV entry factors (EF) were adenovirally delivered to
960 the liver and mice were challenged with HCVcc expressing Cre recombinase
961 (HCV-BiCre-Jc1, genotype 2a). An untreated cohort (*n*=6) was only challenged with HCVcc
962 without adenoviral delivery of human EF. (D) Bioluminescence was quantified 72 hours

following HCV-BiCre-Jc1 infection. Error bars represent SD. Statistical significance was calculated by Kruskal-Wallis One-Way ANOVA analysis: ****, $P<0.0001$.

TABLE 1 NT_{50} of the mouse antisera against HCVcc of genotypes 1-7. The mouse antisera collected at week 27 were pooled for each group and then used for neutralization tests. NT_{50} was defined as the highest dilution of sera able to neutralize 50% of HCVcc infectivity. Data are representative results from three independent experiments.

Antisera	1a	1b			2a		2b	3a	4a	5a	6a	7a
	H77	Con1	PR52 B6mt	PR79 L9	JFH1	J6	J8	S52	ED43	SA13	HK6a	QC69
PBS	<5	<5	<5	<5	<5	<5	<5	<5	<5	<5	<5	<5
sE2+Alum	160	320	160	640	1280	160	80	80	80	160	80	160
sE2+Alum+CpG	320	320	160	640	1280	160	160	160	320	160	160	160
sE2+FA	80	640	160	1280	640	80	80	40	160	80	80	40

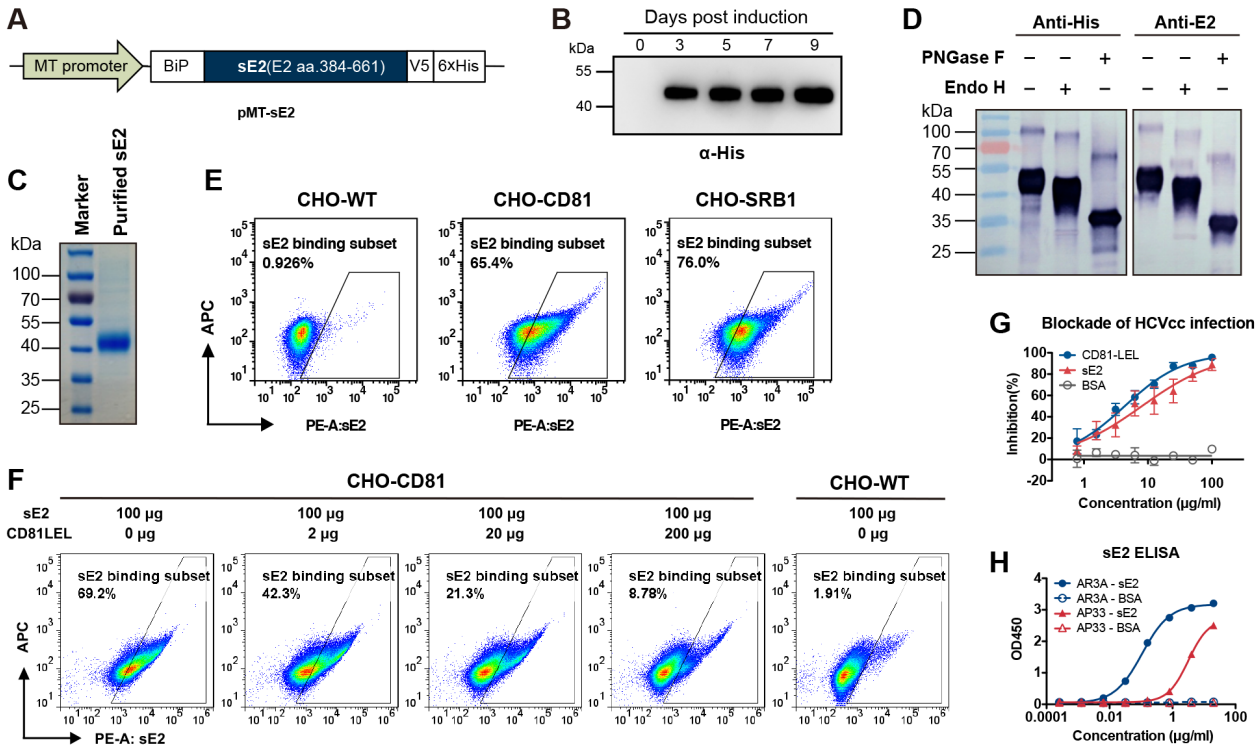

Journal of Virology

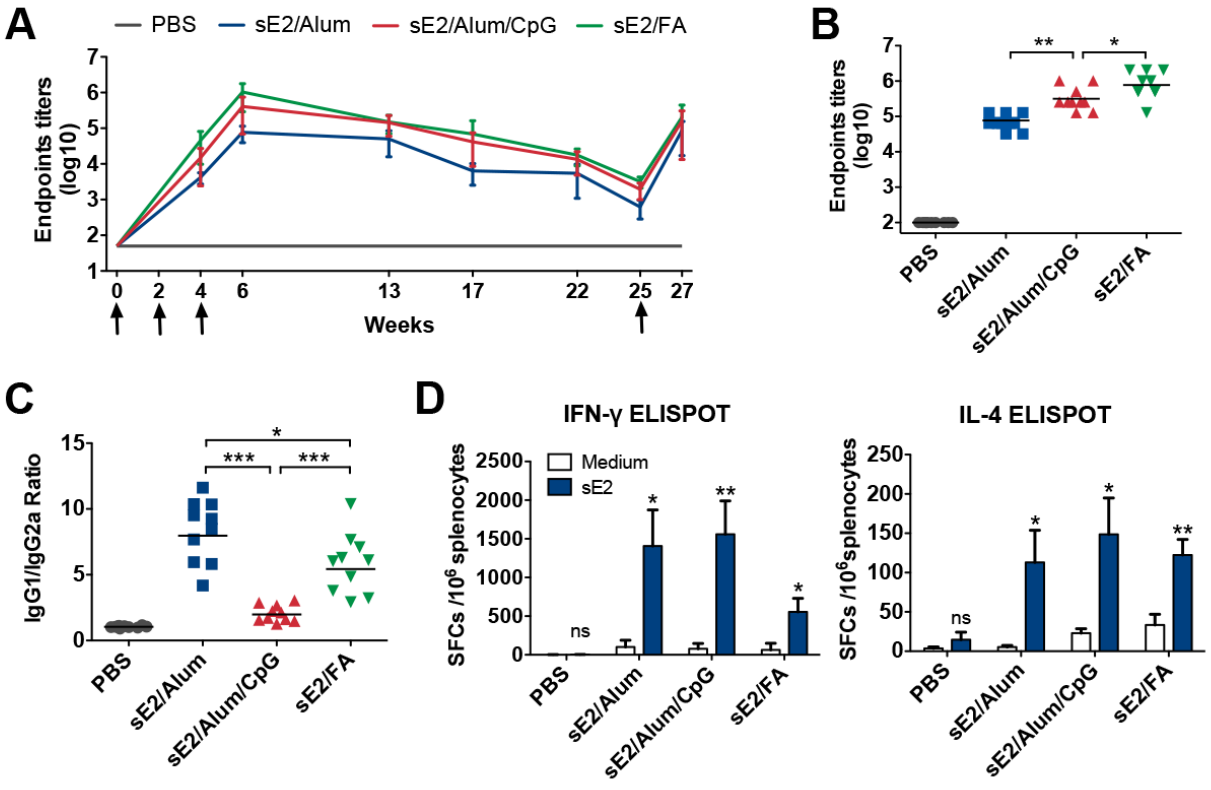

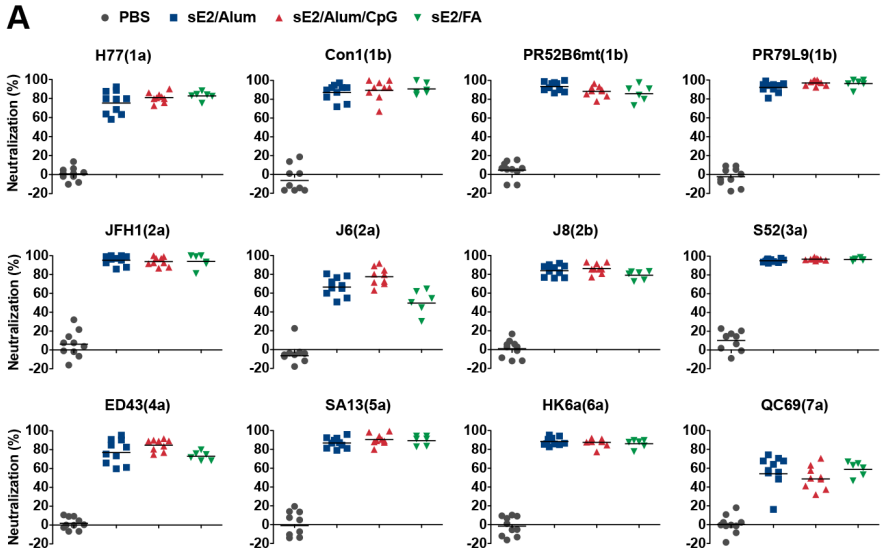

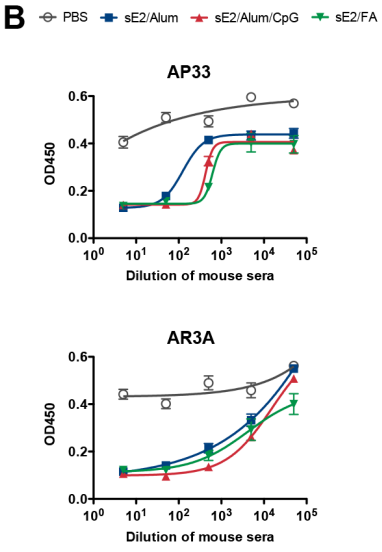

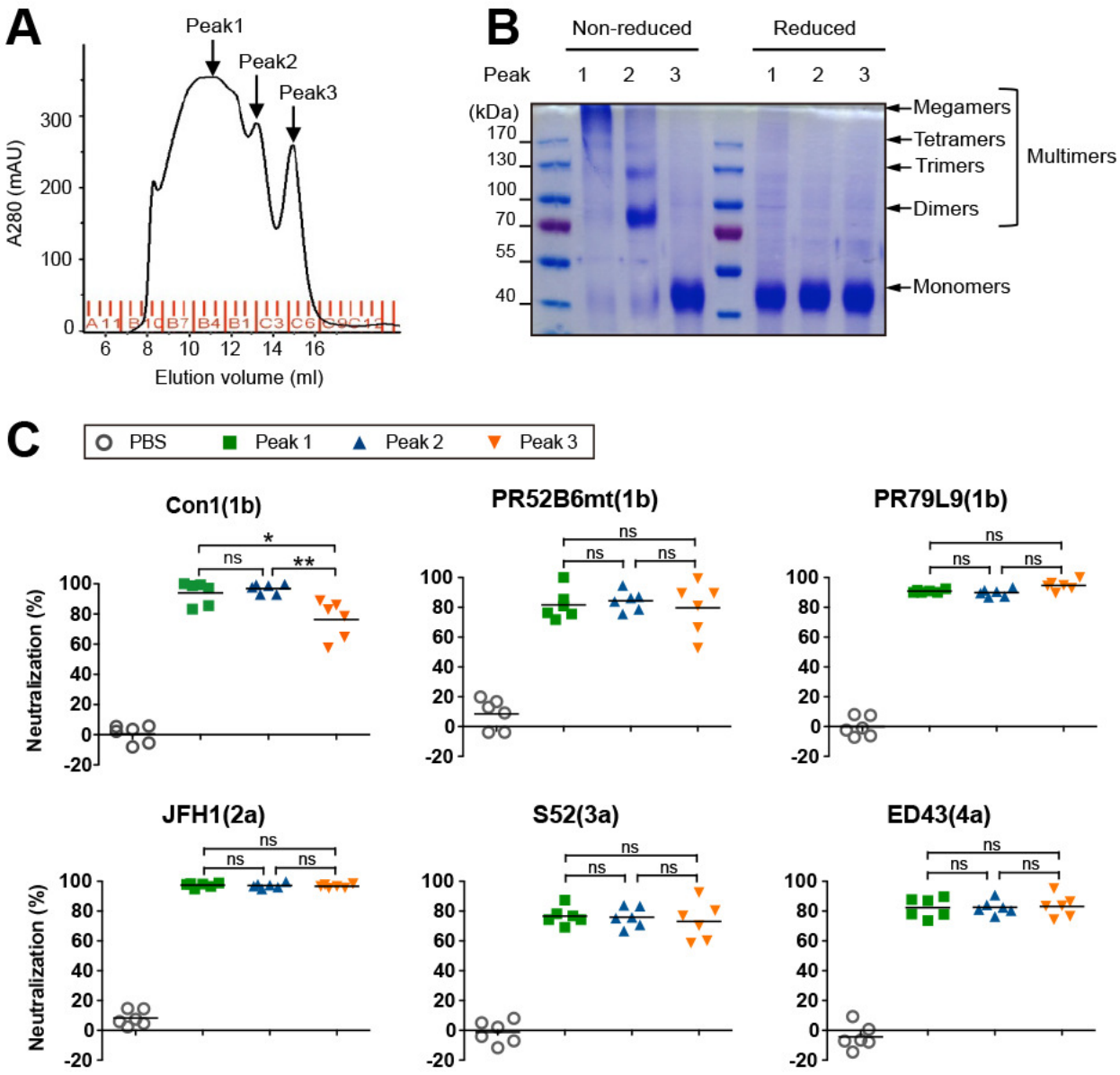

Journal of Virology

JVI

Journal of Virology

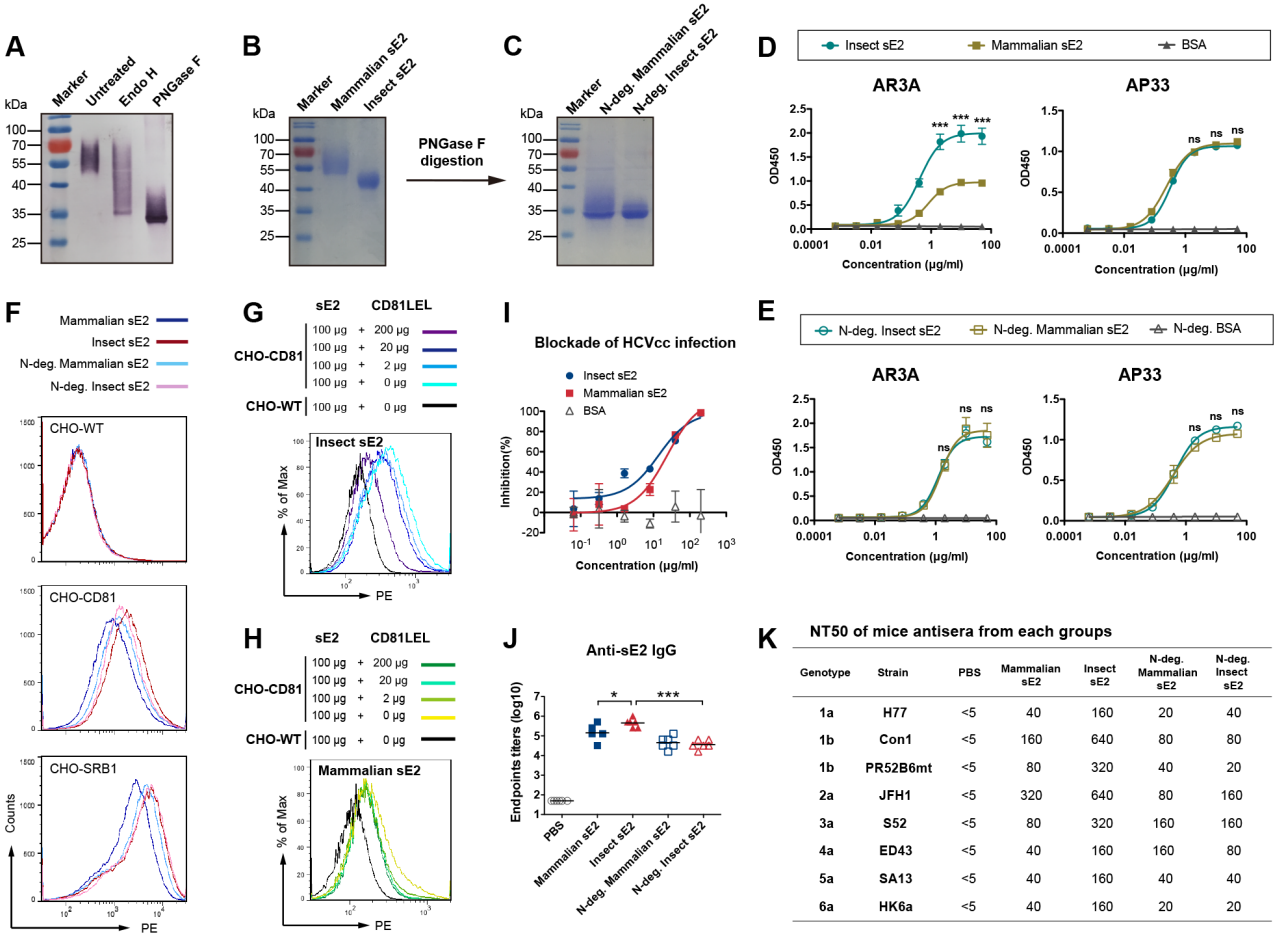

K NT50 of mice antisera from each groups

Genotype	Strain	PBS	Mammalian sE2	Insect sE2	N-deg. Mammalian sE2	N-deg. Insect sE2
1a	H77	<5	40	160	20	40
1b	Con1	<5	160	640	80	80
1b	PR52B6mt	<5	80	320	40	20
2a	JFH1	<5	320	640	80	160
3a	S52	<5	80	320	160	160
4a	ED43	<5	40	160	160	80
5a	SA13	<5	40	160	40	40
6a	HK6a	<5	40	160	20	20